Synthesis, Characterization, Optical Spectroscopic, Electronic Structure, and Second-Order Nonlinear Optical (NLO) Properties of a Novel Class of Donor−Acceptor Bis(salicylaldiminato)nickel(II) Schiff Base NLO Chromophores

Santo Di Bella,*,† Ignazio Fragalà,*,† Isabelle Ledoux,‡ Maria A. Diaz-Garcia,‡,|| and Tobin J. Marks*,§

Contribution from the Dipartimento di Scienze Chimiche, Università di Catania, 95125 Catania, Italy, Molecular Quantum Electronics Department, France Telecom, CNET, 92225 Bagneux, France, and Department of Chemistry and the Materials Research Center, Northwestern University, Evanston, Illinois 60208-3113

Received April 28, 1997[⊗]

Abstract: The synthesis, characterization, thermal stability, optical spectroscopic, electronic structure, and second-order nonlinear optical (NLO) response of a series of donor−acceptor bis(salicylaldiminato)nickel(II) Schiff base complexes and the free ligand precursors are reported. The effect of the metal center in such complexes is manifold: it templates the formation of acentric molecular structures, imparts high thermal stability to the chelate ring, and both "switches on" and enhances NLO response. Metal complexation imparts new linear optical spectroscopic features, having metal-to-ligand charge transfer character, which are responsible for the second-order nonlinearity. Moreover, the present synthetic strategy represents a novel route to inorganic NLO chromophores. Solution-phase hyperpolarizability values, deduced by electric field-induced second-harmonic-generation experiments are as high as -79×10^{-30} cm^5 esu^{-1} ($h\omega = 0.92$ eV). Experimental linear and nonlinear optical features are fully consistent with INDO/SCI-SOS theoretical calculations. They provide a rationale for the NLO response of these materials and are attractive for designing new, highly efficient second-order nonlinear optical inorganic chromophores.

Introduction

Molecule-based second-order nonlinear optical (NLO) materials have recently attracted much interest because they involve new scientific phenomena and because they offer potential applications in emerging optoelectronic technologies.[1−3] Beyond early studies focused on understanding and rationalizing the microscopic molecular nonlinearity, $\beta(-2\omega;\omega,\omega)$, attention has more recently been directed toward optimizing NLO response, toward achieving enhanced chemical and thermal stability, as well as toward improving processability for device fabrication.[1−3] Crucial prerequisites for achieving large bulk second-order NLO responses are that the individual constituents have large molecular responses and that they be arranged in a noncentrosymmetric architecture. Considerable effort has been directed toward the molecular engineering of such structures, and a variety of strategies has emerged. To date, however, this activity has primarily focused on purely organic systems[1−3] and, to a far lesser extent, on organometallic and coordination complexes.[4,5] Compared to organic molecules, metal complexes offer a larger variety of structures, the possibility of high environmental stability, and a diversity of electronic properties tunable by virtue of the coordinated metal center.

We present here a new synthetic strategy for obtaining thermally stable noncentrosymmetric coordination complexes

† Università di Catania.
‡ France Telecom.
§ Northwestern University.
|| Present address: Departamento Materiales C-IV, Universidad Autónoma de Madrid Cantobianco, Madrid 28049, Spain.

⊗ Abstract published in *Advance ACS Abstracts,* September 1, 1997.

(1) (a) *Polymers for Second-Order Nonlinear Optics*; Lindsay, G. A., Singer, K. D., Eds.; ACS Symposium Series 601; American Chemical Society: Washington, DC, 1995. (b) *Molecular Nonlinear Optics*; Zyss, J., Ed.; Academic Press: New York, 1994. (c) Prasad, N. P.; Williams, D. J. *Introduction to Nonlinear Optical Effects in Molecules and Polymers,* Wiley: New York, 1991. (d) *Materials for Nonlinear Optics: Chemical Perspectives;* Marder, S. R., Sohn, J. E., Stucky, G. D., Eds.; ACS Symposium Series 455; American Chemical Society: Washington, DC, 1991. (e) *Nonlinear Optical Properties of Organic Molecules and Crystals*; Chemla, D. S., Zyss, J., Eds.; Academic Press: New York, 1987; Vols 1 and 2.

(2) For recent reviews on NLO materials see, for example: (a) Ledoux, I.; Zyss, J. In *Novel Optical Materials and Applications*; Khoo, I. C., Simoni, F., Umeton, C., Eds; John Wiley & Sons: New York, 1997. (b) Dalton, L. R.; Harper, A. W.; Ghosn, R.; Steir, W. H.; Ziari, M.; Fetterman, H.; Shi, Y.; Mustacich, R. V.; Jen, A. K.-Y.; Shea, K. J. *Chem. Mater.* **1995**, *7*, 1060. (c) Benning, R. G. *J. Mater. Chem.* **1995**, *5*, 365. (c) Marks, T. J.; Ratner, M. A. *Angew. Chem., Int. Ed. Engl.* **1995**, *34*, 155. (d) *Optical Nonlinearities in Chemistry*; Burland, D. M., Ed., *Chem. Rev.* **1994**, *94* (no. 1), 1−278.

(3) (a) *Nonlinear Optical Properties of Organic Materials; Proceedings of SPIE* **1988**−**1994**, Vols. *971, 1147, 1337, 1560, 1775, 2025, 2285*. (b) *Organic Materials for Nonlinear Optics III*; Hann, R. A., Bloor, D., Eds.; Royal Society of Chemistry: London, 1992. (c) *Organic Materials for Nonlinear Optics II*; Hann, R. A., Bloor, D., Eds.; Royal Society of Chemistry: London, 1991. (d) *Organic Molecules for Nonlinear Optics and Photonics*; Messier, J., Kajzar, F., Prasad, P., Eds.; Kluwer Academic Publishers: Dordrecht, 1991. (e) *Organic Materials for Nonlinear Optics*; Hann, R. A., Bloor, D., Eds.; Royal Society of Chemistry: London, 1989.

(4) (a) For a recent review of NLO studies involving organometallic and coordination complexes, see: Long, N. J. *Angew. Chem., Int. Ed. Engl.* **1995**, *34*, 21. (b) For a review including early NLO studies, see: Nalwa, H. S. *Appl. Organomet. Chem.* **1991**, *5*, 349.

(5) For more recent NLO studies on organometallic and coordination complexes see, for example: (a) Cummings, S. D.; Cheng, L. T.; Eisenberg, R. *Chem. Mater.* **1997**, *9*, 440. (b) Di Bella, S.; Fragalà, I.; Marks, T. J.; Ratner, M. A. *J. Am. Chem. Soc.* **1996**, *118*, 12747. (c) Lacroix, P. G.; Di Bella, S.; Ledoux, I. *Chem. Mater.* **1996**, *8*, 541. (d) Houbrechts, S.; Clays, K. Persoons, A.; Cadierno, V.; Gamasa, M. P.; Gimeno, J. *Organometallics* **1996**, *15*, 5266. (e) Whittall, I. R.; Humphrey, M. G.; Houbrechts, S.; Persoons, A.; Hockless, D. C. R. *Organometallics* **1996**, *15*, 5738; 1935. (f) Di Bella, S.; Fragalà, I.; Ledoux, I.; Marks, T. J. *J. Am. Chem. Soc.* **1995**, *117*, 9481. (g) Kanis, D. R.; Lacroix, P. G.; Ratner, M. A.; Marks, T. J. *J. Am. Chem. Soc.* **1994**, *116*, 10089. (h) Bourgault, M.; Mountassir, C.; Le Bozec, H.; Ledoux, I.; Puccetti, G.; Zyss, J. *J. Chem. Soc., Chem. Comm.* **1993**, 1623.

S0002-7863(97)01349-8 CCC: $14.00

Chart 1

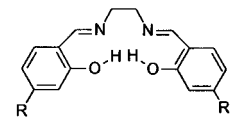

R = H H$_2$(salen) (**1**)
R = OMe H$_2$(4-OMe-salen) (**2**)

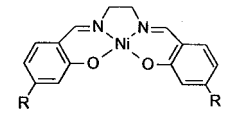

R = H Ni(salen) (**1a**)
R = OMe Ni(4-OMe-salen) (**2a**)

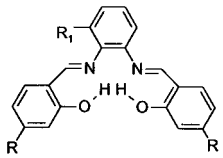

R = H; R$_1$ = H H$_2$(salophen) (**3**)
R = OMe; R$_1$ = H H$_2$(4-OMe-salophen) (**4**)
R = H; R$_1$ = NO$_2$ H$_2$(sal-3-NO$_2$-ophen) (**5**)
R = OMe; R$_1$ = NO$_2$ H$_2$(4-OMe-sal-3-NO$_2$-ophen) (**6**)

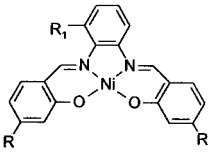

R = H; R$_1$ = H Ni(salophen) (**3a**)
R = OMe; R$_1$ = H Ni(4-OMe-salophen) (**4a**)
R = H; R$_1$ = NO$_2$ Ni(sal-3-NO$_2$-ophen) (**5a**)
R = OMe; R$_1$ = NO$_2$ Ni(4-OMe-sal-3-NO$_2$-ophen) (**6a**)

having sizable second-order NLO responses, tunable by the metal center, and a comparative experimental/theoretical investigation of the molecular second-order NLO properties, $\beta(-2\omega;\omega,\omega)$, of a series of donor−acceptor bis(salicylaldiminato)nickel(II) Schiff base complexes and related ligands (Chart 1).[6] This study focuses on the synthesis, characterization, thermal properties, linear optical spectroscopic, and second-order NLO response, sampled by the electric field-induced second-harmonic-generation (EFISH) technique,[7] in combination with a quantum chemical analysis, within the proven INDO/S-SOS (ZINDO) formalism,[5b,c,e−g,8,9] to describe/understand the electronic structure and structure NLO property relationships of this new class of inorganic NLO chromophores.

Results

Synthesis, Characterization, and Molecular Structure. Schiff base ligands **1**−**6** were prepared in high yields (80−90%) via condensation of the appropriate salicylaldehyde with

Scheme 1

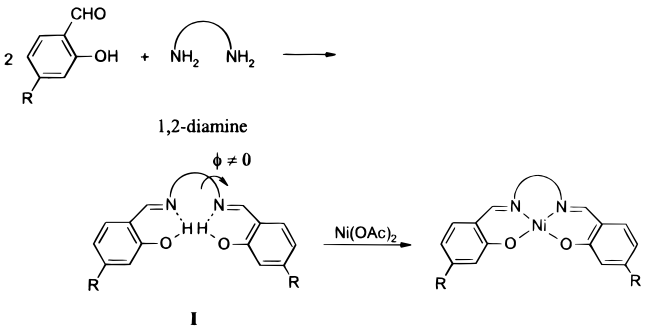

I

the corresponding diamine (Scheme 1; see Experimental Section for details).[10] The yellow imines were readily purified by recrystallization from ethanol. Ligands **1**−**6** were characterized by ^{1}H NMR spectroscopy and satisfactory microanalyses. The crystal structures of unsubstituted H$_2$(salen)[11] (**1**) and H$_2$-(salophen)[12] (**3**) indicate an enolimine tautomeric (nonplanar) structure, also evident in solution.[13] Thus, an analogous, predominantly enoliminic structure (**I** in Scheme 1) can be assumed for the related donor−acceptor substituted imines **2** and **4**−**6**.[14] In support of this formulation, a broad resonance in the low field δ = 12−13 ppm region is evident in the ^{1}H NMR spectra of all the present imine ligands. It disappears upon exchange with D$_2$O and can be associated with the −OH protons doubtless involved in intramolecular hydrogen bonding with iminic nitrogen atoms.

The reaction between ligands **1**−**6** and Ni(II) solutions leads to the formation of stable noncentrosymmetric Ni(II) complexes (**1a**−**6a**; Chart 1, Scheme 1). Yields are 60−70% for **1a**−**4a** and 40−50% for **5a** and **6a**. They were characterized by EI, FAB mass spectrometry, ^{1}H NMR spectroscopy, and satisfactory microanalyses. FAB mass spectra indicate the existence of monomeric species in the gas phase. Furthermore, available X-ray structures of the unsubstituted Ni(salen)[15] (**1a**) and Ni-(salophen)[16] (**3a**) complexes indicate monomeric, planar species in the solid state. Thus, analogous planar, monomeric molecular structures can be safely assumed for the remaining donor−acceptor-substituted Ni(II) complexes **2a** and **4a**−**6a**. Therefore, the formation of planar complexes **1a**−**6a** is expected to effect greater delocalization of out-of-plane π electron density over the chelate and aromatic rings than in the free ligands.

Thermal Analysis. Ligands **1**−**6** exhibit relatively low melting points (120−160 °C). In contrast, complexes **1a**−**6a** are more thermally stable materials which decompose, without melting, at temperatures as high as 380 °C, as judged by combined DSC/TGA thermal analysis (Table 1). The data indicate generally good thermal stability, comparable to or higher than current generation high-efficiency, thermally stable NLO organic chromophores.[17] Within the salophen series, the

(6) (a) For a preliminary communication of some aspects of this work, see: Di Bella, S.; Fragalà, I.; Ledoux, I.; Diaz-Garcia, M. A.; Lacroix, P. G.; Marks, T. J. *Chem. Mater.* **1994**, *6*, 881. (b) Salen coordination polymers have previously investigated for NLO applications: Chiang, W.; Thompson, M. E.; Van Engen, D. In ref 3c, p 210.

(7) For a general discussion of the EFISH tecnique, see: (a) Oudar, J. L. *J. Chem. Phys.* **1977**, *67*, 446. (b) Levine, B, F.; Bethea, C. G. *J. Chem. Phys.* **1976**, *65*, 1989.

(8) Kanis, D. R.; Ratner, M. A.; Marks, T. *J. Chem. Rev.* **1994**, *94*, 195.

(9) (a) There are several definitional issues associated with comparing calculated microscopic responses to those obtained by experiment.[9b] In the present contribution, both derived theoretical and experimental β_μ values employ the Ward definition,[9c] within a perturbation series expansion. (b) Willetts, A.; Rice, J. E.; Burland, D. M.; Shelton, D. P. *J. Chem. Phys.* **1992**, *97*, 7590. (c) Ward, J. F. *Rev. Mod. Phys.* **1965**, *37*, 1.

(10) See, for example: (a) Hoss, H.; Elias, H. *Inorg. Chem.* **1993**, *23*, 317. (b) Chen, D.; Martell, A. E. *Inorg. Chem.* **1987**, *26*, 1026.

(11) Bresciani Pahor, N.; Calligaris, M.; Nardin, G.; Randaccio, L. *Acta Crystallogr.* **1978**, *B34*, 1360.

(12) Bresciani Pahor, N.; Calligaris, M.; Delise, P.; Dodic, G.; Nardin, G.; Randaccio, L. *J. Chem. Soc., Dalton Trans.* **1976**, 2478.

(13) *Comprehensive Coordination Chemistry*; Wilkinson, G., Ed.; Pergamon Press: Oxford, 1987; Vol. 2, p 730.

(14) Although a mixture of three stereoisomers could in principle be formed in the condensation reaction to obtain ligands **4**−**6**, the stereoisomer having both *trans*-imine linkages, i.e., with the enolimine tautomeric structure **I** in Scheme 1, is expected to be predominant. Moreover, since complexation involves only the dianion of stereoisomer **I**, no attempts to separate the mixture of the three stereoisomers were made.

(15) Montgomery, H.; Morosin, B. *Acta Crystallogr.* **1961**, *14*, 551.

(16) Gaetani Manfredotti, A.; Guastini, C. *Acta Crystallogr.* **1983**, *C39*, 863.

Table 1. Experimental[a,b] and ZINDO-Derived Spectroscopic and Nonlinear Optical Properties ($h\omega$ = 0.92 eV) for Donor−Acceptor Schiff Base Ni(II) Complexes and Related Ligands

	λ_{max}, nm		μ_g, D		$\mu\beta$, $\times 10^{-48}$ esu		$\beta\mu$, $\times 10^{-30}$ esu		
compound	exptl ($\epsilon \times 10^{-3}$)	calc (f)	exptl ($\Delta\mu_{ge}$)	calc ($\Delta\mu_{ge}$)	exptl	calc	exptl	calc	T_d[c]
1	318 (8.4)		2.8		0		0		
1a	414 (6.9)	360 (0.26)	8.9 (−3.4)	8.4 (−4.1)	−85	−85	−9.3	−10.1	325
2	308		3.9		4.7		1.2		
2a	398 (8.6)	352 (0.31)	8.6	8.4	−108	−83	−9.6	−12.9	219 (mp)
3	362 (13.4)		6.0		0		0		
3a	480 (9.0)	387 (0.44)	7.0 (−5.1)	8.5 (−5.2)	−147	−144	−20.5	−17.3	360
4	358		5.8		29		5.0		
4a	450 (16.3)	381 (0.50)	5.5	7.5	−126	−165	−23	−22.0	380
5	418		5.9		32		5.5		
5a[d]	570 (9.3)	485 (0.13)	*e*	7.7	−331	−298	−43[f]	−38.7	220
6	420		6.9		54		7.8		
6a[d]	570 (13.1)	491(0.18)	*e*	6.9[g]	−546	−286	−79[f]	−41.5[g]	260

[a] Chloroform solution. [b] Estimated uncertainties are ±5% in μ and ±10% in β_μ. [c] Decomposition temperature (°C) as assessed by the onset of the thermolysis endotherm in the DSC. [d] Acetone solution. [e] Complex insufficiently soluble for accurate measurement. [f] Estimated using calculated dipole moment. [g] The calculated μ and β_μ values for compound **6a** differ from those previously reported[6a] because of the different conformation presently adopted for the 4-OMe substituents (vide infra).

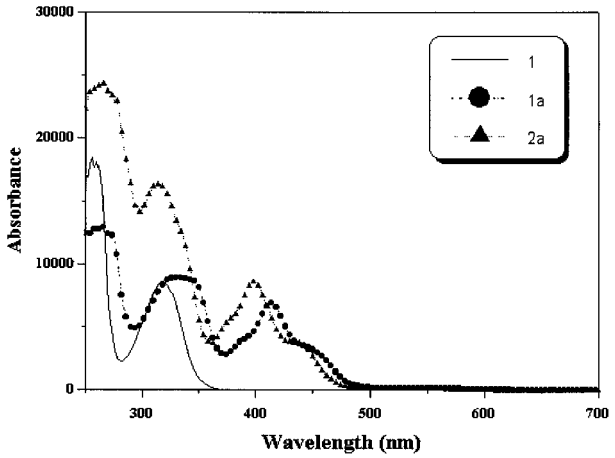

Figure 1. Optical absorption spectra of H_2(salen) and complexes **1a** and **2a** in chloroform solution.

present thermal stabilities increase with 4-methoxysalicylidene ring substitution and decrease with 3-nitrophenylene ring substitution.

Optical Spectroscopy. The solution-phase optical absorption spectrum (>280 nm) of ligand **1** consists (Figure 1) of a relatively intense band centered at 318 nm (ϵ = 8400), involving $\pi\rightarrow\pi^*$ transitions,[18] and of a low intensity feature ($\epsilon \approx 100$) in the 380−420 nm region, responsible for the yellow color, and presumably involving $n\rightarrow\pi^*$ excitation.[18] Complexation with Ni(II) results in two overlapping principal features assigned[19] to two different types of transitions. There is a broader band in the region between 300 and 360 nm still involving principally intraligand $\pi\rightarrow\pi^*$ transitions and a new, relatively intense structure in the 380−480 nm region, absent in the absorption spectrum of the free ligand, involving both the ligand and the metal center. Moreover, the band at 414 nm (ϵ = 6900) exhibits a significant solvatochromic shift, characteristic of a large dipole moment change ($\Delta\mu$) between the ground and the excited state, and indicative of charge transfer (CT) character. In particular, a negative solvatochromism, i.e., a hypsochromic (blue) shift with increasing solvent polarity, is observed (Table 2), indicating a reduction in the dipole moment upon electronic excitation ($\Delta\mu$ = −3.4; Table 1). Finally, a weak feature ($\epsilon \approx 100$) assigned to "d−d" transitions,[19] is present in the 500−600 nm region (Figure 1).

Table 2. Optical Absorption Maxima of the Lowest Energy Charge-Transfer Optical Transition for Ni(salen) and Ni(salophen) Complexes in Solvents Having Different Polarities

	λ_{max}, nm					
complex	CCl_4	benzene	chloroform	ethyl acetate	acetone	methanol
Ni(salen)		422	414	414	410	400
Ni(salophen)	494	488	480	480	478	466

The 4-methoxy substitution of the salicylidene rings (H_2(4-OMe-salen), **2**) results in a new, relatively intense band in the longer wavelength region (388 nm) and in a more intense and blue-shifted absorption band at 308 nm, compared to the 318 nm band of **1**. This alteration is reflected in the optical spectrum of **2a**, which is slightly blue-shifted and more intense than that of **1a** (Figure 1). Substitution of the ethylenediamine bridge of **1** with *o*-phenylenediamine (**3**) effects a larger π charge delocalization over the salicylidene and phenylene aromatic rings than in **1**, resulting in a more intense, broader and red-shifted $\pi\rightarrow\pi^*$ band in the optical spectrum (Figures 1 and 2). This structural modification is also reflected in the optical spectrum of Ni(II) complex **3a** which exhibits two new intense features in the longer wavelength region (a band at 381 nm and structure in the 420−550 nm region), the latter of which is more intense and red-shifted compared to that of Ni(salen) (Figures 1 and 2). Moreover, in analogy to **1a**, the band centered at 480 nm (ϵ = 9000) in **3a** exhibits an analogous negative solvatochromism (Table 2), but a stronger dipole moment change ($\Delta\mu$ = −5.1, Table 1), thus indicating greater CT character of the associated optical transition.

Either 4-methoxy substitution in the salicylidene fragment, or 3-NO_2 substitution in the phenylene fragment of the salophen ligand series (**4**−**6**), results in a new spectroscopic structure in the longer wavelength region (a relatively intense shoulder at 440 nm for **4** and an intense band at ∼420 nm for **5** and **6**). These substituent modifications are in turn reflected in the optical spectra of **5a** and **6a** which exhibit new spectral features in the 500−600 nm region, compared to that of the unsubstituted **3a** complex (Figure 2). In contrast, the longer wavelength band in the optical spectrum of **4a** is slightly blue-shifted, but substantially more intense, compared to that of **3a** (Figure 2).

Ground-State Dipole Moment. Ground-state dipole moments, μ_g, of the present ligands and Ni(II) complexes measured

(17) See, for example: Moylan, C. R.; Twieg, R. J.; Lee, V. Y.; Swanson, S. A.; Betterton, K. M.; Miller, R. D. *J. Am. Chem. Soc.* **1993**, *115*, 12599.
(18) Crawford, S. M. *Spectrochim. Acta* **1963**, *19*, 255.
(19) Bosnich, B. *J. Am. Chem. Soc.* **1968**, *90*, 627.

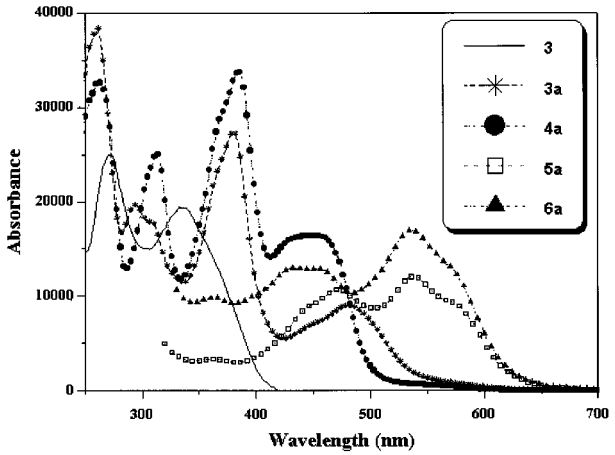

Figure 2. Optical absorption spectra of H_2(salophen) and complexes **3a**−**6a** in chloroform (**3**, **3a**, **4a**) or acetone (**5a**, **6a**) solution.

in chloroform solution are collected in Table 1. Within the salen series, the dipole moments of ligands **1** and **2** are consistently lower than the corresponding values of Ni(II) complexes **1a** and **2a**. This is consistent with a pseudo-centrosymmetric structure of the free salen ligands (trans conformation with respect to the ethylenediamine bridge),[11] which becomes constrained and noncentrosymmetric in the subsequent Ni(II) complexes, thus resulting in an increased dipole moment. However, for the present salophen series in which a noncentrosymmetric enoliminic structure is expected (vide infra), complexation actually results in a smaller dipole moment change. In both complexes of the salen and salophen series, salicylidene ring 4-methoxy substitution results in a smaller dipole moment with respect to the unsubstituted species.

Second-Order NLO Response. The molecular hyperpolarizabilities, $\beta(-2\omega;\omega,\omega)$, of the present compounds were measured by the EFISH technique.[7,20] This technique allows the determination of the $\mu\cdot\beta$ dot product when an electric field is applied to a solution of an NLO-active species. The β_μ value, i.e., the vector component of the β_{ijk} tensor along the dipole moment direction,[21] can be thus extracted if the ground-state dipole moment is known. Experimental β_μ values of the present ligands and complexes are compared in Table 1. It can be seen that complexation dramatically enhances and, in some cases, "switches on" the second-order NLO response. The β_μ values of **1a**−**6a** are rather large for coordination complexes,[4,5] ranging from $\sim -10 \times 10^{-30}$ cm^5 esu^{-1} ($h\omega = 0.92$ eV), similar to that of the classical donor−acceptor organic chromophore *p*-nitroaniline,[22] to $\sim -79 \times 10^{-30}$ cm^5 esu^{-1}, rivaling β_μ values reported for efficient, second-order organic chromophores such as 4,4′-donor−acceptor-substituted stilbenes.[22] The observed NLO response along the **1a**−**6a** series parallels the aforementioned red-shift and intensity increase of the lowest CT excitation, as usually observed in typical donor−acceptor organic chromophores.[23]

EFISH measurements on unsubstituted ligands **1** and **3** indicate a vanishingly small NLO response, while for substituted ligands **2** and **4**−**6**, positive β_μ values, $\sim$$^1/_5$ to $^1/_7$ the magnitude of the related Ni(II) complexes, are observed. These observations illustrate the efficacy of metal complexation in "switching on" and tuning the NLO response, upon formation of noncentrosymmetric structures.

Table 3. INDO Eigenvalues and Mulliken Population Analysis of the Outermost MO's for Ni(salen)

		population, %					
MO	ϵ, eV	Ni	2O	2N	2C$_{im}$[a]	12C$_{sal}$[b]	character[b]
62	1.87	51	8	12	5	24	d_{xy}
59	1.21	0	4	0	0	96	C_{sal}
58	1.19	0	4	0	2	94	C_{sal}
57	−0.47	2	4	20	38	36	C═N
56[c]	−0.51	1	2	22	36	39	C═N
55[d]	−7.49	13	22	10	0	55	d_{xz}, O_{2p}
54	−7.94	5	18	2	1	74	O_{2p}, C_{sal}
53	−8.45	35	5	11	0	49	d_{yz}, N_{2p}, C_{sal}
52	−8.55	60	13	3	0	24	d_{z^2}
51	−8.68	7	1	9	1	82	d_{xz}, C_{sal}
50	−9.57	42	4	1	4	49	d_{yz}, C_{sal}

[a] C_{im} = imine carbon atoms. [b] C_{sal} = salicylidene carbon atoms. [c] LUMO. [d] HOMO.

Theoretical Results. Electronic Structure and Optical Spectroscopy. The electronic structure of the H_2(salen) ligand **1** can be described in terms of two weakly interacting *N*-salicylideneamine subunits. The frontier molecular orbitals (MO's) of the latter molecule consists of symmetry combinations of filled out-of-plane O_{2pz}, π_2 benzene, and π C═N imine orbitals and of unfilled π^* C═N MO's.

The metal−ligand bonding in the present Ni(II) complexes can be described analogously to that of d^8 square-planar complexes studied previously.[24] Thus, the metal−ligand bonding involves metal 3d, 4s, 4p valence orbitals and more external filled MO's of the ligand dianion. The latter consist of in-plane N_{2p} and O_{2p} lone pairs and of out-plane π_2 benzene, π C═N and O_{2pz} orbitals of appropriate symmetry combinations (a_2 and b_2 in C_{2v}). All these orbitals are strongly admixed and perturbed by the interaction with the metal ion; however, the net metal−ligand stabilization arises from the σ donation of the in-plane N_{2p} and O_{2p} lone pairs to the empty metal $3d_{xy}$,4s orbitals.

INDO eigenvalues and atomic population analyses of the frontier MO's for prototypical Ni(salen) (**1a**) are reported in Table 3. They consist of out-of-plane π orbitals mainly delocalized over the salicylidene rings which have some C═N and O_{2pz} contributions, admixed to varying extents with metal 3d orbitals of appropriate symmetry. In particular, the HOMO and SHOMO possess a large O_{2pz} contribution, while the LUMO and SLUMO possess a predominant C═N character. The calculated ground-state dipole moment (8.4 D) is in very good agreement with the experimental value (8.9 D; Table 1) and is directed between the imine groups (Scheme 2). INDO/S calculations account well for the experimental linear optical spectroscopic features, and a satisfactory agreement between calculated and observed transition energies is found (Table 4). In particular, the aforementioned band at 414 nm may be characterized as principally $\pi\rightarrow\pi^*$ (HOMO→LUMO) in character, essentially involving the metal d_{xz} + O_{2pz} and the C═N orbitals, and is mainly responsible for the second-order NLO response (vide infra). Moreover, the calculated negative $\Delta\mu_{ge}$ (−4.1 D) value associated with this transition is in good agreement with that determined from the negative solvatochromism (−3.4 D; Table 1).

On passing to Ni(salophen) (**3a**), substitution of the ethylenediamine bridge of **1a** with the phenylenediamine ring leads

(20) (a) Ledoux, I.; Zyss, *J. Chem. Phys.* **1982**, *73*, 203. (b) Barzoukas, M.; Josse, D.; Fremaux, P.; Zyss, J.; Nicoud, J. -F.; Morley, J. O. *J. Opt. Soc. Am. B* **1987**, *4*, 977.

(21)
$$\beta_\mu(-2\omega;\omega,\omega) = \sum_{i=1}^{3}\frac{\mu_i\beta_i}{|\mu|}$$

where $\beta_i = \beta_{iii} + {}^1/_3\sum_{j\neq i}(\beta_{ijj} + \beta_{jij} + \beta_{jji})$.

(22) Cheng, L. -T.; Tam, W.; Stevenson, S. H.; Meredith, G. R.; Rikken, G.; Marder, S. R. *J. Phys. Chem.* **1991**, *95*, 10631.

(23) Di Bella, S.; Marks, T. J.; Ratner, M. A. *J. Am. Chem. Soc.* **1994**, *116*, 4440.

(24) See, for example: Di Bella, S.; Casarin, M.; Fragalà, I.; Granozzi, G.; Marks, T. J. *Inorg. Chem.* **1988**, *27*, 3993.

Table 4. Comparison of INDO/S-Derived[a] and Experimental Optical Transition Energies[b] of Ni(salen)

exc state	λ^{calc}	f^{calc} [c]	λ_{max}^{expt}	f^{expt} [c]	composition[d] of CI expansion	principal character
S1	422	0.008	540	0.00	$-0.68\chi^{52\rightarrow62} + 0.39\chi^{53\rightarrow62}$ $+0.35\chi^{55\rightarrow57}$	$d_{z2}d_{xy}$
S2	368	0.043	446	0.03	$0.38\chi^{52\rightarrow62} + 0.35\chi^{54\rightarrow56}$ $-0.45\chi^{55\rightarrow56}$ $0.56\chi^{55\rightarrow57}$	d_{xz}, $O_{2p}C{=}N$
S3	364	0.029			$-0.39\chi^{48\rightarrow62} + 0.37\chi^{49\rightarrow62}$ $+0.26\chi^{51\rightarrow62} - 0.32\chi^{55\rightarrow56}$ $0.64\chi^{55\rightarrow62}$	d_{xz}, $O_{2p}d_{xy}$
S4	360	0.257	414	0.07	$-0.41\chi^{54\rightarrow57} - 0.62\chi^{55\rightarrow56}$ $-0.53\chi^{55\rightarrow57}$	d_{xz}, $O_{2p}C{=}N$
S5	342	0.005	392 (sh)		$+0.59\chi^{50\rightarrow62} + 0.27\chi^{52\rightarrow62}$ $+0.60\chi^{53\rightarrow62}$	$d_{yz}d_{xy}$
S8	293	0.508	332	0.15	$-0.27\chi^{51\rightarrow56} + 039\chi^{51\rightarrow57}$ $0.38\chi^{53\rightarrow56} + 0.54\chi^{54\rightarrow56}$	$\pi\pi^*$
S11	277	0.180			$-0.32\chi^{50\rightarrow56} + 0.43\chi^{52\rightarrow56}$ $0.55\chi^{53\rightarrow56}$	d_{z^2}, $d_{yz}C{=}N$

[a] Singlet excited states (S). [b] Transition energies (λ_{max}) in nm. [c] Oscillator strength. [d] See Table 3.

Scheme 2

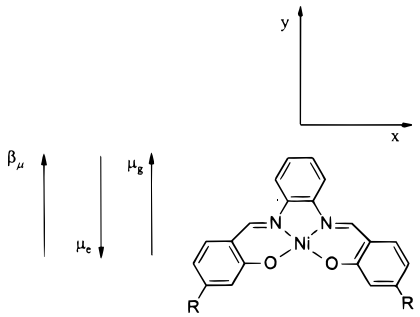

1a-4a

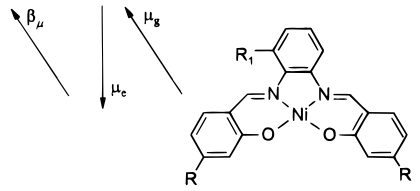

5a, 6a

to a larger π charge delocalization over the entire molecule, and the frontier MO's acquire a significant phenylene ring character. This is reflected in a reduced energy gap between the frontier MO's as well as in a calculated and observed red shift of the lowest CT transition (**1a** vs **3a**; Table 1). In addition, both the observed and calculated intensity and dipole moment change associated with this transition are larger compared to those of Ni(salen) (Table 1), because of the increased π charge delocalization over the phenylene ring.

The 4-methoxy donor substitution in the salicylidene rings and/or the 3-NO_2 acceptor substitution in the phenylene ring results in some donor character of the frontier filled MO's and a dominant acceptor character of the lowest unoccupied MO's. This, in turn, leads to a larger energy gap between filled and unoccupied MO's in the case of **4a** and in a reduced gap for complexes **5a** and **6a**, which is also reflected in stronger calculated blue- and red-shifted lowest energy CT transitions for **4a** and **5a** + **6a**, respectively, in agreement with the experimental data (Table 1).

The 4-methoxy substitution in the salicylidene rings of **3a** leads to a lower calculated total dipole moment in **4a**, in agreement with the experiment (Table 1). Since the dipole moment is directed between the imine groups, substitution of an electron-donor group such as the methoxy in the salicylidene rings tends to balance the charge separation with respect to the unsubstituted complex, thus resulting in a reduced dipole moment (see Scheme 2). Moreover, note that while in the C_{2v}-symmetric complexes **1a**−**4a**, the total dipole moment (μ_g) is oriented along the *y* axis (i.e., $\mu_g = \mu_y$) and, in turn along the μ_e CT axis, in the asymmetrically 3-NO_2 substituted complexes **5a** and **6a**, the μ_g and μ_y vectors are not parallel, since the μ_x vector component also makes an appreciable contribution (Table 5, Scheme 2).

Second-Order Molecular Nonlinearity. The calculated second-order hyperpolarizabilities[5,8,9] of the present molecules are collected in Table 1 and compared with the experimental data. The agreement between experimental and theoretical values is very good in terms of both absolute values as well as in the trends observed within the series.

For C_{2v} complexes **1a**-**4a**, the dominant contribution to β_μ derives from the *yyy* component of the β_{ijk} hyperpolarizability tensor (where *y* is the direction along the principal dipole moment axis of the molecule), which is parallel to the CT axis (Scheme 2). In contrast, for unsymmetrical 3-NO_2 substituted complexes **5a** and **6a**, μ_g and μ_e are not parallel and while β_{yyy} is still the largest tensor, the $\beta_{xxy} = \beta_{xyx}$ tensors also contribute significantly to the nonlinearity, and the total hyperpolarizability (β_{vec})[25] is substantially larger than β_μ (Table 5).

In accord with experiment, an almost vanishing nonlinearity ($\beta_\mu = 0.4 \times 10^{-30}$ cm^5 esu^{-1}; $h\omega = 0.92$ eV; on the basis of the crystal structure[11]) is calculated for the H_2(salen) ligand, even assuming a cis (relative to the ethylene bridge) conformation. Analogously, in the case of unsubstituted H_2(salophen), the small calculated β_μ value (0.9×10^{-30} cm^5 esu^{-1}; $h\omega =$ 0.92 eV; assuming the distorted crystal structure[12]) agrees well with the observed vanishing β_μ. In addition, even assuming an idealized planar structure, a small β_μ value (3.1×10^{-30} cm^5 esu^{-1}; $h\omega = 0.92$ eV) is still predicted. This observation further underscores the effect of the metal center in "switching on" the NLO response, because of a greater π charge delocalization over the chelate ring and the existence of new excited states created upon metal coordination.

Discussion

Metal complexation of ligands **1**−**6** with Ni(II) leads to formation of thermally stable, constrained acentric planar

(25) $\beta_{vec} = (\beta_x^2 + \beta_y^2 + \beta_z^2)^{1/2}$. Note that β_{vec} is always a positive quantity regardless of the sign of the individual vectorial β_i components.

Table 5. Computed Second-Order NLO Response[a] and Hyperpolarizability-Determining Parameters (eq 1) for Donor−Acceptor Schiff-Base Ni(II) Complexes

compd	μ_x, D	μ_y, D	μ_g, D	state[b]	$h\omega_{eg}$, eV	r_{ge}, D	$\Delta\mu_{ge}$, D	$\beta_{yyy,t}$	β_{yyy}	β_μ	β_{vec}	$\beta_{0,vec}$[c]
1a	0.0	8.4	8.4	S4	3.44	4.36	−4.1	−5.6	−6.9	−10.1	10.1	7.6
2a	0.0	8.4	8.4	S3	3.52	4.70	−3.7	−6.0	−7.2	−12.9	12.9	9.8
3a	0.0	8.5	8.5	S2	3.21	5.97	−5.2	−18.2	−16.1	−17.3	17.3	11.5
4a	0.0	7.5	7.5	S2	3.26	6.38	−4.9	−17.6	−17.3	−22.0	22.0	15.1
5a	4.8	6.1	7.7	S3	2.55	3.58	−10.7	−29.5	−52.6	−38.7	59.0	27.3
6a	4.8	5.0	6.9	S2	2.52	4.10	−11.6	−43.0	−58.8	−41.5	68.7	32.5
7a	0.0	19.4	19.4	S4	3.01	5.99	0.2	0.7	3.8	14.2	14.2	7.6
8a	3.2	1.9	3.7	S3	3.12	6.16	−6.6	−33.0	−43.8	−14.5	55.6	31.7
9a	0.0	0.22	0.22	S3	2.09	5.88	14.9	373.0	424.8	447.6	447.6	88.0

[a] In 10^{-30}cm^5 esu^{-1} ($h\omega$ = 0.92 eV). [b] S = singlet excited state involved in the two-state contribution. [c] Total static (zero frequency) hyperpolarizability.

structures **1a**−**6a**, which possess new linear optical features responsible for the pronounced second-order optical nonlinearity. The effect of the metal center is thus manifold: it templates the formation of acentric structures, imparts high thermal stability to the chelate ring, and both "switches on" and enhances the NLO response. Moreover, the good agreement between NLO experimental and theoretical data for the present complexes suggests that theory can be used with confidence in rationalizing nonlinearity and in designing new molecular architectures having optimized NLO response.

A detailed analysis of the computational results indicates that the second-order NLO response of the present complexes is dominated in all instances by the intense, low-energy HOMO → LUMO CT excitation mentioned above, in which the metal acts as a electron donor. In such cases, the quadratic hyperpolarizability can be simply related to the two-state contribution (eq 1),[7a] where $h\omega$ is the incident (laser) radiation frequency,

$$\beta_{yyy}(-2\omega;\omega,\omega) = \frac{3e^2}{2}\frac{h\omega_{eg}r_{ge}^2\,\Delta\mu_{ge}}{((h\omega_{eg})^2-(h\omega)^2)((h\omega_{eg})^2-(2h\omega)^2)} \quad (1)$$

and $h\omega_{eg}$, r_{ge}, and $\Delta\mu_{ge}$, are, respectively, the energy, the transition dipole moment, and the dipole moment variation, between the ground and first CT excited state. Therefore, the increasing β_μ values observed on passing from **1a** to **6a** can be directly related to the increasing CT character, hence, greater $\Delta\mu_{ge}$ values and to the bathochromic shift of the β-determining CT transition (Table 5).

The negative experimental and calculated β_μ values are a consequence of the experimental and calculated negative solvatochromism, hence negative $\Delta\mu_{ge}$ values, associated with the β-determining CT transition (eq 1). This is due to a different orientation of the dipole moment on passing from the ground to the excited state. In particular, while in the ground state the dipole moment is directed between the imine groups, in the excited state it has an opposite orientation, i.e., between the oxygen donor atoms (Scheme 2). The larger NLO response of substituted donor−acceptor complexes **4a**−**6a** with respect to unsubstituted Ni(salophen) (**3**) results from an accurate design of ring substitution in order to maximize $\Delta\mu_{ge}$, i.e., the CT character of the relevant optical transition. For example, an inverted ring-substitution pattern in **3**, that is 4-NO_2 acceptor substitution in the salicylidene rings (**7a**) instead of in the phenylene ring, would increase the ground-state dipole moment but would decrease the CT character of the lowest optical transition and, hence, the nonlinearity (Table 5). On the other hand, 4-NO_2 (instead of 3-NO_2) phenylene ring substitution in Ni(salophen) (**8a**) results (**8a** vs **5a**) in a lower ground-state dipole moment and a smaller $\Delta\mu_{ge}$ associated with the involved lowest CT transition, in addition to an increased oscillator strength and a blue shift of the same transition. The balancing effects of these contributions leads to a slightly smaller β_{vec} than for 3-NO_2, but to a substantially smaller β_μ (Table 5).

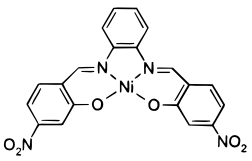

7a

These observations have interesting implications for the design of donor-acceptor metal complex architectures having optimized NLO response. For example, the combination of a stronger (than the methoxy) 4-donor substituent in the salicylidene rings, such as the diethylamino group, and 3,6-NO_2 phenylene ring substitution, leads to a donor-acceptor structure (**9a**) which is predicted (Table 5) to possess an almost vanishing dipole moment ($\mu_g = \mu_y = 0.22$ D, having an opposite direction than in **4a**−**8a**), but a very large CT character ($\Delta\mu_{ge}$ = 14.9 D) and a *very large* NLO response ($\beta_\mu \cong \beta_{yyy} = 448 \times 10^{-30}$ cm^5 esu^{-1}; $h\omega$ = 0.92 eV; $\beta_0 = 88.0 \times 10^{-30}$ cm^5 esu^{-1}).[26]

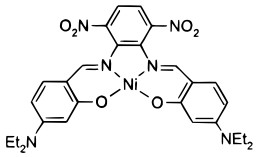

9a

Conclusions

This paper presents the synthesis and characterization of a novel class of thermally stable, geometrically constrained acentric NLO inorganic chromophores the second-order response of which is "switched on" and tuned by the coordination of a metal center. Even if the NLO response of these new materials is modest compared to latest generation organic NLO chromophores,[2a−c] the present synthetic strategy represents a novel route to metal−organic NLO chromophores which are intriguing candidates for further studies and applications.[27]

Experimental Section

Starting Materials. Salicylaldehyde, 2-hydroxy-4-methoxybenzaldehyde, ethylenediamine, and nickel(II) acetate tetrahydrate (reagent grade, Aldrich) were used without further purification. 1,2-Phenylene-

(26) In this case, positive $\Delta\mu_{ge}$ and β_μ values are computed because the ground- and excited-state dipole moments are both directed between the oxygen donor atoms.

(27) (a) Preliminary studies indicate that they can be easily incorporated in thermally stable main-chain polymers for poled polymer NLO applications.[27b] (b) Vitalini, D.; Mineo, P.; Di Bella, S.; Fragalà, I.; Maravigna, P.; Scamporrino, E. *Macromolecules* **1996**, *29*, 4478.

diamine and 3-nitro-1,2-phenylenediamine (Aldrich) were purified by sublimation in vacuo.

Synthesis of Ligands and Complexes. All Schiff bases were prepared using standard procedures[10] involving reaction of the appropriate salicylaldehyde with the corresponding diamine (2:1 molar ratio) in ethanol. The yellow imines were purified by recrystallization from ethanol (yields 80−90%). The complexes were prepared[10,28] by reaction of an aqueous (for **1a**−**4a**) or methanolic (for **5a** and **6a**) solution of nickel(II) acetate with a boiling alcoholic solution of the corresponding Schiff base ligand (1:1 molar ratio). The precipitated complexes were collected by filtration, washed with an H_2O/ethanol mixture, and then recrystallized from absolute ethanol and/or chloroform (yields, 60−70%). In the case of complexes **5a** and **6a**, the precipitates were washed with methanol (yields 40−50%). While complexes **1a**−**4a** are soluble in most common organic solvents, **4a** and **5a** are soluble in strongly polar solvents and moderately soluble in acetone.

H_2(salen) (1). Melting point: 125−126 °C. Anal. Calcd for $C_{16}H_{16}N_2O_2$: C, 71.62; H, 6.01; N, 10.44. Found: C, 71.40; H, 5.98; N, 10.02.

Ni(salen), 1a. Anal. Calcd for $C_{16}H_{14}N_2O_2Ni$: C, 59.13; H, 4.34; N, 8.62. Found: C, 58.99; H, 4.30; N, 8.29.

H_2(4-OMe-salen) (2). Melting point: 162−163 °C. ^{1}H NMR (250 MHz, $CDCl_3$): δ 3.79 (s, 4H, CH_2), 3.85 (s, 6H, OMe), 6.34−6.41 (m, 4H, Ph), 7.08 (d, J = 8.00 Hz, 2H, Ph), 8.20 (s, 2H, CH═N), 13.74 (br, s, 2H, OH). Anal. Calcd for $C_{18}H_{20}N_2O_4$: C, 65.84; H, 6.14; N, 8.53. Found: C, 65.41; H, 5.99; N, 8.15.

Ni(4-OMe-salen) (2a). Melting point: 217−219 °C. EI MS (70 eV) *m/z*: 384, 386 (M^+). ^{1}H NMR (250 MHz, $CDCl_3$): δ 3.35 (s, 4H, CH_2), 3.74 (s, 6H, OMe), 6.16 (dd, J = 8.7, 2.5 Hz, 2H, Ph), 6.51 (d, J = 2.4 Hz, 2H, Ph), 6.91 (d, J = 8.7, 2H, Ph), 7.29 (s, 2H, CH═N). Anal. Calcd for $C_{18}H_{18}N_2O_4Ni$: C, 56.15; H, 4.71; N, 7.27. Found: C, 55.82; H, 4.50; N, 6.93.

H_2(salophen) (3). Melting point: 164−165 °C. ^{1}H NMR (250 MHz, DMSO-d_6): δ 6.9−7.0 (m, 4H, Ph), 7.3−7.6 (m, 8H, Ph), 8.85 (s, 2H, CH═N), 13.02 (br, s, 2H, OH). Anal. Calcd for $C_{20}H_{16}N_2O_2$: C, 75.93; H, 5.10; N, 8.85. Found: C, 75.80; H, 4.99; N, 8.71.

Ni(salophen) (3a). FAB MS (3NBA) *m/z*: 373 (MH^+). ^{1}H NMR (250 MHz, DMSO-d_6): δ 6.67 (t, J = 7.3 Hz, 2H, Ph), 6.88 (d, J = 8.5 Hz, 2H, Ph), 7.33 (m, 4H, Ph), 7.60 (d, J = 8.0 Hz, 2H, Ph), 8.15 (dd, J = 6.2, 3.0 Hz, 2H, Ph), 8.90 (s, 2H, CH═N). Anal. Calcd for $C_{20}H_{14}N_2O_2Ni$: C, 64.39; H, 3.78; N, 7.51. Found: C, 64.01; H, 3.70; N, 7.32.

H_2(4-OMe-salophen) (4). Melting point: 167−168 °C. ^{1}H NMR (250 MHz, $CDCl_3$): δ 3.83 (s, 6H, OMe), 6.45−6.55 (m, 4H, Ph), 7.22−7.32 (m, 6H, Ph), 8.54 (s, 2H, CH═N), 13.62 (s, 2H, OH). Anal. Calcd for $C_{22}H_{20}N_2O_4$: C, 70.20; H, 5.35; N, 7.44. Found: C, 69.89; H, 5.31; N, 7.15.

Ni(4-OMe-salophen) (4a). FAB MS (3NBA) *m/z*: 433 (MH^+). ^{1}H NMR (250 MHz, $CDCl_3$): δ 3.80 (s, 6H, OMe), 6.32 (dd, J = 8.89, 2.43 Hz, 2H, Ph), 7.15−7.22 (m, 4H, Ph), 7.65 (dd, J = 7.65, 3.33, Hz, 2H, Ph), 8.09 (s, 2H, CH═N). Anal. Calcd for $C_{22}H_{18}N_2O_4$: C, 61.01; H, 4.19; N, 6.47. Found: C, 60.69; H, 3.98; N, 6.18.

H_2(sal-3-NO_2-ophen) (5). Melting point: 156−158 °C. ^{1}H NMR (250 MHz, DMSO-d_6): δ 6.72 (t, J = 8.10 Hz, 2H, Ph), 7.0 (m, 3H, Ph), 7.4−7.5 (m, 3H, Ph), 7.8−8.0 (m, 3H, Ph), 8.91 (s, 2H, CH═N), 11.75 (br, s, 2H, OH). Anal. Calcd for $C_{20}H_{15}N_3O_4$: C, 66.48; H, 4.18; N, 11.63. Found: C, 66.01; H, 3.98; N, 11.20.

Ni(sal-3-NO_2-ophen) (5a). FAB MS (3NBA) *m/z*: 418 (MH^+). ^{1}H NMR (250 MHz, DMSO-d_6): δ 6.32 (t, J = 7.5 Hz, 2H, Ph), 6.69 (t, J = 7.5 Hz, 1H, Ph), 6.82 (d, J = 8.1 Hz, 2H, Ph), 7.38 (m, 2H, Ph), 7.59 (d, J = 7.5 Hz, 1H, Ph), 7.72 (d, J = 8.3 Hz, 2H, Ph), 7.92 (d, J = 7.1 Hz, 1H, Ph), 8.31 (s, 2H, CH═N). Anal. Calcd for $C_{20}H_{13}N_3O_4$-Ni: C, 57.46; H, 3.13; N, 10.05. Found: C, 56.9; H, 3.26; N, 9.82.

H_2(4-OMe-sal-3-NO_2-ophen) (6). Melting point: 176−178 °C. ^{1}H NMR (250 MHz, DMSO-d_6): δ 3.81 (s, 6H, OMe), 6.50−6.75 (m, 5H, Ph), 7.36 (dd, J = 7.45, 1.37 Hz, 1H, Ph), 7.72 (d, J = 8.62 Hz, 2H, Ph), 7.91 (dd, J = 8.71, 1.36 Hz, 1H, Ph), 8.78 (s, 2H, CH═N), 12.22 (br, s, 2H, OH). Anal. Calcd for $C_{22}H_{19}N_3O_6Ni$: C, 62.70; H, 4.54; N, 9.97. Found: C, 62.40; H, 4.32; N, 9.61.

Ni(4-OMe-sal-3-NO_2-ophen) (6a). EI MS (70 eV) *m/z*: 477, 479 (M^+). ^{1}H NMR (250 MHz, DMSO-d_6) δ 3.75 (s, 6H, OMe), 6.2−6.4 (m, 5H, Ph), 7.45 (d, J = 8.6 Hz, 1H, Ph), 7.64 (d, J = 8.6 Hz, 2H, Ph), 7.80 (d, J = 7.3 Hz, 1H, Ph), 8.32 (s, 2H, CH═N). Anal. Calcd for $C_{22}H_{17}N_3O_6Ni$: C, 55.26; H, 3.58; N, 8.79. Found: C, 54.9; H, 3.48; N, 8.48.

Physical Measurements. Elemental analyses were performed on a Carlo Erba 1106 elemental analyzer. EI and FAB mass spectra were recorded on a Kratos MS 50 double-focusing mass spectrometer equipped with a standard FAB source. FAB MS spectra were obtained by using 3-nitrobenzyl alcohol (3NBA) as the matrix. ^{1}H NMR spectra were recorded on a Bruker AC-250 spectrometer. Thermal measurements were performed with a Mettler 3000 system equipped with a TG 50 thermobalance, a TC 10 processor, and a DSC 30 calorimeter. The weight of samples was 15−20 mg for thermogravimetric analysis (TGA), and 4−8 mg for differential scanning calorimetry (DSC). Thermal analyses were made under prepurified nitrogen using a 10 °C/min heating rate. Thermal stabilities were estimated by combined DSC and TG analyses. The intercept of the leading edge of the decomposition endotherm with the base line of each DSC scan was assigned as the decomposition temperature (T_d).[17] At this T_d, the corresponding weight loss in each thermogram was always less than 2%.

Spectroscopy. UV−vis spectra were recorded with a Beckman DU 650 spectrophotometer, and λ_{max} values are considered accurate to ±1 nm. Optical absorption spectra of complexes **1a**−**4a** in chloroform solution, recorded in the 5×10^{-3} to 2×10^{-6} M range, followed the Lambert−Beer law, thus indicating that the complexes were monomeric in solution.

The dipole moment variation between the ground and the excited state, $\Delta\mu_{ge}$, was determined from the solvatochromism of the relevant absorption band by means of the Lippert−Mataga equation[29] where

$$\nu_{cr} = \nu_{CT}^{g} + C_1\frac{n^2-1}{2n^2+1} + C_2\left(\frac{D-1}{D+2} - \frac{n^2-1}{n^2+2}\right) \qquad (2)$$

ν_{CT} is the frequency (cm^{-1}) of the optical transition in a particular solvent, D and n are the dielectric constant and refractive index of the solvent, respectively. The intercept, ν_{CT}^{g}, is the frequency of the transition in the gas phase, and $C_2 = 2\mu_g\Delta\mu_{ge}/hca^3$; where μ_g is the ground-state dipole moment, h and c are Planck's constant and the speed of light, respectively, a is the Onsager radius, and $\Delta\mu_{ge}$ is the dipole moment change. The constant C_2 was determined from the least-squares fit of eq 4 to the absorption maxima of the CT band in 13 different solvents. $\Delta\mu_{ge}$ was calculated from C_2 with the measured value of the ground-state dipole moment and a value of the Onsager radius (6.0 Å and 6.5 Å for **1a** and **3a**, respectively) estimated from the solute molar volume.[23]

EFISH Measurements. Second-order molecular hyperpolarizability analyses were performed using a Q-switched mode-locked Nd:YAG laser operating at 1.34 μm ($h\omega$ = 0.92 eV) by the electric field-induced second-harmonic-generation method.[20] The laser delivers pulse trains of total duration envelope around 90 ns, each pulse duration being 160 ps. The molecules to be measured were dissolved in chloroform (used as a reference) or acetone (for complexes **5a** and **6a**) at various concentrations, x, between 5×10^{-3} and 5×10^{-4} M, and the solutions were placed in the wedge-shaped measurement cell. A high voltage pulse (around 5 kV), synchronized with the laser pulse, breaks the centrosymmetry of the liquid by dipolar orientation of the molecules. Translation of this cell perpendicular to the beam direction modulates the second-harmonic signal into Maker fringes. The amplitude and periodicity of the fringing pattern are related to the macroscopic susceptibility, $\Gamma(x)$, of the solution and to the coherence length, $l_c(x)$. Calibrations were made with respect to the pure solvent. $\Gamma(x)$ is related to the microscopic hyperpolarizability of the solvent, γ_s, and of the dissolved molecule, γ_m, by

(28) Olszewski, E. J.; Martin, D. F. *J. Inorg. Nucl. Chem.* **1964**, *26*, 1577.

(29) Mataga, N.; Kubota, T. *Molecular Interactions and Electronic Spectra;* Marcel Dekker: New Work, 1970; p 371.

$$\Gamma(x) = \frac{Nf\rho}{1+x}\left(\frac{\gamma_s}{M_s} + x\frac{\gamma_m}{M_m}\right) \quad (3)$$

where ρ is the density of the solvent, N is Avogrado's number, f is an averaged local field factor, and M_s and M_m are the molecular masses of the solvent and of the solute, respectively. γ_m is given by

$$\gamma_m = \gamma_e + \frac{\mu_g \cdot \beta_\mu}{5kT} \quad (4)$$

where γ_e is the scalar part of the third-order hyperpolarizability, μ_g the ground-state dipole moment, and $\beta_\mu = \beta_{yyy} + \beta_{yxx} + \beta_{yzz} \approx \beta_{yyy}$ for one-dimensional charge-transfer molecule. In this work, we have neglected the small γ_e contribution. The sign of β_μ was determined by studying the variation of $\Gamma(x)$ as a function of x. If β_μ is negative, Γ first decreases when increasing x and then cancels out when the contribution from the solvent is exactly compensated by that of the dissolved NLO molecule. The $\Gamma(x)$ value then increases because it is dominated by the contribution of the solute. Further details of the experimental methodology and data analysis are reported elsewhere.[20]

The ground-state dipole moment was determined by the standard method of Guggenheim.[30]

Theoretical Methods. The all-valence INDO/S (intermediate neglect of differential overlap) formalism,[31] in connection with the sum-over excited particle-hole-states (SOS) formalism,[5b,8] was employed. Details of the computationally-efficient ZINDO-SOS-based method for describing second-order molecular optical nonlinearities have been reported elsewhere.[5b,8] Standard parameters and basis functions were used.[31] In the present approach, the closed-shell restricted Hartree−Fock (RHF) formalism was adopted. The monoexcited configuration interaction (CIS) approximation was employed to describe the excited states. In all calculations, the lowest 160 energy transitions between SCF and CIS electronic configurations were chosen to undergo CI mixing and were included in the SOS. This SOS truncation was found to be sufficient for complete convergence of the second-order response in all cases considered. All calculations were performed using the ZINDO program[5b,8] implemented on an IBM ES/9000 system.

Metrical parameters used for the calculations were taken from related crystal structure data.[15,16] Standard bond distances and bond angles were adopted for donor−acceptor substituents.[32] A *syn* conformation of methoxy groups with respect the C_{sal}−OMe bonds was adopted for substituted 4-OMe **2a**, **4a**, and **6a** complexes.[33] This conformation was found always to be more stable than the *anti* one. Calculations were performed assuming a C_{2v} planar (pseudo-planar for **1a** and **2a**; local C_{2v} for asymmetrically 3-NO_2 substituted complexes **5a** and **6a**) geometry. In the case of free ligands **1**−**6**, no attempts to perform a complete conformational analysis were made, thus no calculated spectroscopic and NLO data were reported, except those for unsubstituted **1** and **3** species, for which the crystallographic structure was assumed.[11,12]

Acknowledgment. This research was supported by the Consiglio Nazionale delle Ricerche (CNR Rome), by the Ministero dell'Università e della Ricerca Scientifica e Tecnologica (MURST, Rome), by the NSF-MRL Program through the Materials Research Center of Northwestern University (Grant DMR9632427) and by the MURI program of the DOD through the CAMP research collaboration (ONR N00014-95-1-1319. We thank Dr. P. G. Lacroix (CNRS, Toulouse) for helpful discussions and Professor F. Castelli (Università di Catania) for thermal measurements.

JA971349Y

(30) Guggenheim, E. A. *Trans. Faraday Soc.* **1949**, *45*, 203.

(31) (a) Zerner, M.; Loew, G.; Kirchner, R.; Mueller-Westerhoff, U. *J. Am. Chem. Soc.* **1980**, *102*, 589. (b) Anderson, W. P.; Edwards, D.; Zerner, M. C. *Inorg. Chem.* **1986**, *25*, 2728. (b) Bacon, A. D.; Zerner, M. C. *Theor. Chim. Acta (Berlin)* **1979**, *53*, 21. (c) Ridley, J.; Zerner, M. C. *Theor. Chim. Acta (Berlin)* **1973**, *32*, 111.

(32) Kanis, D. R.; Marks, T. J.; Ratner, M. A. *Int. J. Quantum Chem.* **1992**, *43*, 61.

(33) In the previously reported calculations[6a] on **6a**, an *anti* conformation was adopted, thus resulting in a slightly different calculated NLO response.